Smart Structures and Systems, *Vol. 18, No. 3 (2016) 501-523*
DOI: http://dx.doi.org/10.12989/sss.2016.18.3.501

Piezoelectric impedance based damage detection in truss bridges based on time frequency ARMA model

Xingyu Fan, Jun Li* and Hong Hao

Centre for Infrastructural Monitoring and Protection, School of Civil and Mechanical Engineering, Curtin University, Kent Street, Bentley, WA6102, Australia

(Received December 15, 2015, Revised February 8, 2016, Accepted March 17, 2016)

Abstract. Electromechanical impedance (EMI) based structural health monitoring is performed by measuring the variation in the impedance due to the structural local damage. The impedance signals are acquired from the piezoelectric patches that are bonded on the structural surface. The impedance variation, which is directly related to the mechanical properties of the structure, indicates the presence of local structural damage. Two traditional EMI-based damage detection methods are based on calculating the difference between the measured impedance signals in the frequency domain from the baseline and the current structures. In this paper, a new structural damage detection approach by analyzing the time domain impedance responses is proposed. The measured time domain responses from the piezoelectric transducers will be used for analysis. With the use of the Time Frequency Autoregressive Moving Average (TFARMA) model, a damage index based on Singular Value Decomposition (SVD) is defined to identify the existence of the structural local damage. Experimental studies on a space steel truss bridge model in the laboratory are conducted to verify the proposed approach. Four piezoelectric transducers are attached at different locations and excited by a sweep-frequency signal. The impedance responses at different locations are analyzed with TFARMA model to investigate the effectiveness and performance of the proposed approach. The results demonstrate that the proposed approach is very sensitive and robust in detecting the bolt damage in the gusset plates of steel truss bridges.

Keywords: structural damage detection; piezoelectric impedance; time-frequency ARMA; steel bridge; gusset; joint condition

1. Introduction

In the last several decades, structural health monitoring techniques have been developed with system identification and damage detection approaches to evaluate the safety condition of civil infrastructure. As one of the widely used smart materials, piezoelectric ceramic (PZT) material, which transforms the energy between mechanical deformation and electricity, has been developed as a transducer patch that can be attached on the structural surface to monitor the structural health conditions. The electromechanical impedance (EMI) based structural health monitoring technique is rapidly developing in the recent years. Those techniques have been successfully applied to monitoring structural systems, i.e., beam and plate like structures. In the study by Raju *et al.*

*Corresponding author, Senior Lecturer, E-mail: : junli@curtin.edu.au; LI.Jun@connect.polyu.hk

http://www.techno-press.org/?journal=sss&subpage=8 ISSN: 1738-1584 (Print), 1738-1991 (Online)

(1998), PZT patches were attached on a composite reinforced concrete wall to detect the structural failure under loading. Sohn *et al.* (2003) investigated the EMI technique on a simulated three-story moment resisting frame structure, and monitored the bolt loosening on the brackets. Park *et al*. (2008) implemented the k-mean clustering–based unsupervised pattern recognition from the electromechanical impedance-based wireless SHM system to detect bolt loosen in a bolt-jointed aluminum structure. Wang *et al*. (2007) presented to use the impedance characteristics to detect the crack in a Timoshenko beam structure. Park *et al*. (2005) presented the results of a feasibility study on an impedance-based damage detection technique using thickness modes of PZT patches for steel structural members. Pavelko *et al*. (2014) applied EMI technique on Mi-8 helicopter tail beam to monitor the condition of its bolt-joints. The frequency domain impedance responses were compared between the undamaged and damaged structures to detect the damage existence. Sun *et al.* (2015) presented the debonding identification method for RC beams strengthened with FRP based on PZT impedance transducers. Experimental study on concrete strength monitoring based on embedded PZT transducer was carried out by Wang *et al*. (2014).

PZT has been applied to various structures, i.e., beams, frames and plates for the purpose of structural health monitoring in the abovementioned studies. In this paper, the main focus is trying to investigate the feasibility and possibility of using PZT for the condition monitoring of gusset plates in steel truss bridges. Gusset plates are the key connections ensuring the safety and functionality of steel truss bridges. Potential damage in gusset plate might cause severe collapse of steel truss bridges. In 2007, the bridge carrying Interstate Highway 35W (I-35W, National Bridge Inventory Structure No. 9340) over the Mississippi River in Minneapolis, suffered a sudden tragic collapse within a second. According to the post-accident investigation, a total of 111 vehicles were on the collapsed portion. More than 17 vehicles fell into the water. Thirteen people died, and a hundred and forty five people were injured because of the collapse. The investigation led by the National Transportation Safety Board (2008) indicated that a damaged gusset plate under the concentrated loading area was the main reason to this collapse as shown in Fig. 1, and concluded that regular loading rating and annual visual inspections may not be able to adequately detect the gusset plate conditions. There is an emerging need to perform effective structural condition monitoring on the gusset plate in steel truss bridges. Time-frequency analysis methods, such as wavelet analysis and Hilbert-Huang Transform (HHT), are popular and well adopted in structural health monitoring (Yang *et al.* 2003, Yang *et al.* 2004, Rucka and Wilde 2006, Yi *et al.* 2013a, b, Li *et al*. 2014, Li and Hao 2014). The merits of time-frequency analysis methods are based on their ability to reflect both time and frequency domain information (Li and Hao 2015). Impedance based structural health monitoring technique with a time-frequency analysis method is investigated in this study as one of the potential approaches which can be applied to the damage detection in gusset plates of steel truss bridges.

This paper presents a new structural damage detection approach based on analyzing the time domain impedance responses from piezoelectric transducers. The measured time domain responses from the piezoelectric transducers will be directly used for the analysis. With the use of the Time-Frequency Autoregressive Moving Average (TFARMA) model, a Singular Value Decomposition (SVD) based damage index is defined to detect the damage. The effectiveness and performance of the proposed approach are investigated by experimental studies on a space steel truss bridge model in the laboratory. Four pieces of piezoelectric transducers are placed at different locations on the bridge model and excited by a sweep-frequency signal. The time domain impedance responses are analyzed with TFARMA model to calculate the damage index. The TFARMA damage index will be compared with other two traditional EMI based damage indices with frequency domain impedance to demonstrate the superiority of the proposed approach.

2. Background of conventional impedance based damage detection methods

PZT is a kind of piezoelectric materials, which is commonly used as EMI transducer. The PZT transducer is able to generate a voltage output when compressed or the applied electric field can be transferred to a physical shape change. When using EMI based techniques for structural health monitoring, PZT patches are bonded on the surface of the monitored structures and exited directly by an alternating voltage sweep signal with a signal generator or an impedance analyzer. With the basic electromechanical model of a bonded PZT, which is presented by Liang *et al.* (1994), we have

$$Y(\omega) = \frac{I}{V} = i\omega a(\bar{\varepsilon}_{33}^{T} - \frac{Z(\omega)}{Z(\omega)+Z_a(\omega)} d_{3x}^{2} \hat{Y}_{xx}^{E}) \tag{1}$$

Assuming that the mechanical properties of the PZT patch is not varying during the monitoring period, any changes in the structural dynamic properties would be indicated by the changes in the electrical impedance signature of PZT transducers. The changes in impedance signals from bonded PZT transducers may be analyzed and used to calculate some statistical index to detect the damage. Conventionally, statistical deviation of raw measured impedance signals in the frequency domain is calculated to define an index for structural damage detection, such as root mean square deviation (RMSD) expressed as follows (Naidu 2004)

$$RMSD = \sqrt{\frac{\sum_{j=1}^{N}(G_j^1 - G_j^0)^2}{\sum_{j=1}^{N}(G_j^0)^2}} \tag{2}$$

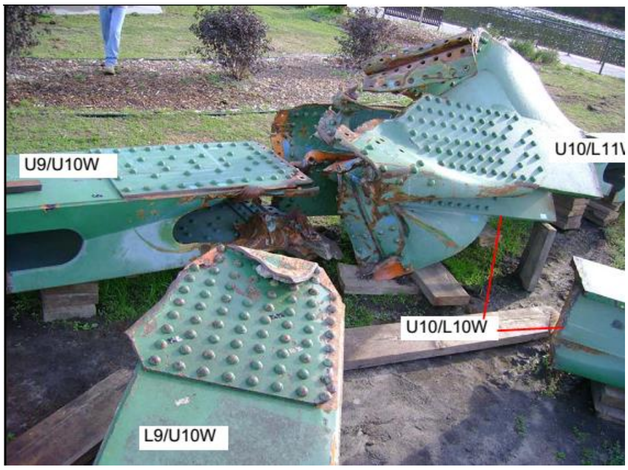

Fig. 1 The failure node U10 in I-35W bridge (National Transportation Safety Board, 2008)

where G_j^1 and G_j^0 denote the impedance signals of PZT patch at the *j*-th frequency line from

the damaged and healthy strucutres, respectively.
Correlation Coefficient (CC) is another damage index which is widely used in the EMI based technique. It is defined as the covariance of two impedance response data divided by the product of their standard deviations. The defination of CC is given as (Tseng and Naidu 2002)

$$CC = 1 - \frac{Cov(x, y)}{\sigma_x \sigma_y} \tag{3}$$

where σ_x and σ_y denote the standard deviations of impedance signals of PZT transducer in the undamaged and damaged states, respectively. CC indicates the linear relationship betwee two impedance signals in a similar manner as covariance.

Conventional damage detection approaches based on impedance signals are performed by comparing the measured frequency domain impedance responses from the healthy and damaged structures in order to detect the structural changes with respect to the baseline structure. RMSD and CC damage indices as shown in Eqs. (2) and (3) respectively are two of those typically and widely recognized approaches in EMI based structural health monitoring techniques. Such damage indices are easy to compute and can be used to indicate the occurrence of structural damage, however, their sensitivity to detect the local minor damage, especially in the large-size complex structures, is a significant issue and concern.

3. Methodology of the proposed approach

3.1 TFARMA model

The theoretical background of TFARMA model is briefly presented here. A structural damage detection approach based on TFARMA model analysis is proposed with a SVD-based damage index. The main difference between the traditional damage indices, i.e., RMSD and CC presented in Section 2, and the proposed damage index is that the presented study analyzes and represents the impedance data through TFARMA model in a multiple dimensional space. By analyzing the measured time domain impedance signals with TFARMA, the feasibility, sensitivity and performance of the proposed approach will be investigated.

The impedance signal from a PZT transducer is a non-stationary random process. The parametric models for random processes, such as auto-regressive (AR), moving average (MA), and Auto-regressive Moving Average (ARMA), are well known and have been applied to signal analysis and system identification. Jachan *et al*. (2007) presented the TFARMA model for non-stationary random processes. Both time delays and Doppler frequency shifts are added to the time invariant ARMA models. The TFARMA model which reveals the non-stationary and the spectral correlation is given as (Feng *et al.* 2013)

$$x(n) = -\sum_{m=1}^{M_A} \sum_{l=-L_A}^{L_A} a_{m,l} \exp(j\frac{2\pi}{N}nl) x(n-m) + \sum_{m=1}^{M_B} \sum_{l=-L_B}^{L_B} b_{m,l} \exp(j\frac{2\pi}{N}nl) e(n-m) \tag{4}$$

where *e(n)* is the stationary white noise with a variance equal to 1, M_A, L_A, M_B and L_B are the model orders. The time-varying AR parameters $a_m(n)$ and MA parameters $b_m(n)$ are expressed as finite order Fourier basis expansions

$$a_m(n) = \sum_{l=-L_A}^{L_A} a_{m,l} \exp(j\frac{2\pi}{N} nl) \tag{5}$$

$$b_m(n) = \sum_{l=-L_B}^{L_B} b_{m,l} \exp(j\frac{2\pi}{N} nl) \tag{6}$$

In this TFARMA model, the under-spread process is applied to obtain the results of non-stationary process with small high-lag temporal and spectral correlations. The substance of this process is to assume the lags of the time–frequency shifts to be small values. As a result, the proposed TFARMA model is effective for detecting the slowly varying components of signals.

3.2 TFMA and TFAR parameters

TFMA parameters $b_{m,l}$ can be estimated by a recursive algorithm based on complex time-frequency cepstrum, which is expressed as

$$b_{m,l} \approx \frac{1}{N} \sum_{m'=0}^{m-1} \sum_{l'=-L_B}^{L_B} \frac{m-m'}{m} b_{m',l'} C(m-m', l-l') \tag{7}$$

with the initialization

$$b_{0,l} \approx \frac{1}{N} F_{n\to l} \exp\left[\frac{1}{2} F_{l'\to n}{}^{-1} C(0,l')\right] \tag{8}$$

where $m = 1,\cdots, M_B$, $l = -L_B,\ldots, L_B$, $F_{\to}(\cdot)$ and $F_{\to}^{-1}(\cdot)$ represent Fourier transform and inverse Fourier transform, respectively. The complex time-frequency cepstrum is described as

$$C(m,l) = F_{k\to m}{}^{-1} F_{n\to l} \log\left[F_{m'\to k} F_{l'\to n}{}^{-1} A(m',l')\right] \tag{9}$$

The ambiguity function is given as

$$A_x(m,l) = F_{n\to l}\, x(n) x^*(n-m) \tag{10}$$

Under the underspread condition, TFAR parameters $a_{m,l}$ can be estimated based on the underspread time–frequency Yule–Walker equations (Stoica and Moses 1997), which is given as

$$\sum_{m'=1}^{M_A} \sum_{l'=-L_A}^{L_A} a_{m',l'} A(m-m', l-l') = -A(m,l) \tag{11}$$

where $m = 1,\ldots, M_A$ and $l = -L,\ldots, L_A$.

3.3 TFARMA parameters

TFARMA model parameters can be estimated by combining the above estimations of parameters $a_{m,l}$ and $b_{m,l}$. Under the underspread condition, parameters $a_{m,l}$ for the TFAR part can be calculated by the Wax–Kailath algorithm (Wax and Kailath1983) which is given as

$$\sum_{m'=1}^{M_A}\sum_{l'=-L_A}^{L_A} a_{m',l'} A_x(m-m',l-l') = -A_x(m,l) \tag{12}$$

where $m = 1+M_B,.....,M_A+M_B$, $l = -L_A,.....L_A$.

For the TFAM part, the parameter $b_{m,l}$ can be obtained by the following recursive algorithm

$$\begin{aligned} b_{m,l} = \frac{1}{N}\sum_{m'=0}^{m-1}\sum_{l'=-L_A}^{L_A}\frac{m-m'}{m}A_x(m-m',l-l')\sum_{m''=0}^{m'}\sum_{l''=-L_A}^{L_A}\frac{m-m'}{m}a_{m'',l''}b_{m'-m'',l'-l''} \\ +\sum_{m'=1}^{m-1}\sum_{l'=-L}^{L}\frac{m-m'}{m}(a_{m-m',l-l'}b_{m',l'} - a_{m',l'}b_{m-m',l-l'}) + \sum_{l'=-L_A}^{L_A} a_{m,l'}b_{0,l-l'} \end{aligned} \tag{13}$$

where $m = 1,...,M_B$, $l = -L_B,...,L_B$, and $L = \max(L_A, L_B)$

When the TFARMA parameters are estimated, the order of the TFARMA model can be calculated by an information criterion through minimizing the following AIC function

$$AIC(M_A, L_A, M_B, L_B) = \log\left[\frac{1}{N}\sum_{n=0}^{N-1}\left|\hat{e}(n)\right|^2\right] + \frac{2}{N}\left[M_A(2L_A+1)+(M_B+1)(2L_B+1)-1\right] \tag{14}$$

3.4 TFARMA evolutionary spectrum

To visualize the TFARMA model parameters and provide a better demonstration for the damage detection, the evolutionary spectrum is calculated from the estimated TFARMA model parameters. The evolutionary spectrum of the TFARMA process is defined by (Jachan *et al*. 2005)

$$P[n,k] \stackrel{\Delta}{=} \frac{|B[n,k]|^2}{|A[n,k]|^2} \tag{15}$$

where

$$A[n,k] = \sum\nolimits_{(m,l)\in \mathrm{A}} a_{m,l}\, e^{j\frac{2\pi}{N}(nl-km)} \tag{16}$$

$$B[n,k] = \sum\nolimits_{(m,l)\in \mathrm{B}} b_{m,l}\, e^{j\frac{2\pi}{N}(nl-km)} \tag{17}$$

A and B denote the delay-Doppler support regions that were given by

$\mathrm{A} \stackrel{\Delta}{=} \{1,...,M_A\} \times \{-L_A,...,L_A\}$ and $\mathrm{B} \stackrel{\Delta}{=} \{0,...,M_B\} \times \{-L_B,...,L_B\}$. M_A and M_B represent the TFAR and TFMA delay orders, L_A and L_B represent TFAR and TFMA Doppler order, respectively.

3.5 Damage index based on TFARMA model analysis

A damage index is defined based on analyzing the characteristics of the evolutionary spectra from TFARMA model analysis. To compare the evolutionary spectra of the healthy and damaged responses from PZT transducers, SVD is applied to identify the pattern of the evolutionary spectrum and it can be expressed as

$$SVD(spectrum^T) = U_{i*j} S_{j*j} V_{j*j} \tag{18}$$

where the singular values are given by the diagonal elements of the matrix *S*. The largest singular value corresponding to the first column vector in the matrix *U* reflects the most important principal component of the spectrum, that is, the largest singular value and its associated vector can be used to reveal the characteristics of the evolutionary spectrum.

Base on the SVD results, the damage index from TFARMA model analysis is defined as

$$\text{TFARMA damage index} = \frac{\|D - H\|}{\|H\|} \tag{19}$$

where *H* and *D* denote the first column vectors in the matrix *U* from the SVD of the evolutionary spectrum under the healthy and the damaged conditions, respectively. This damage index quantifies the correlation between the evolutionary spectra from the healthy and damaged structures. Both the damage indices as shown in Eqs. (2), (3) and (19) have a value from zero to unity, where zero means that the measured responses have a very close correlation and the structure is in the health condition, however, unity means that the measured responses have a very bad correlation and the structure is in a severe damage situation. Those three damage indices are used to identify the structural conditions. The effectiveness of the proposed approach will be demonstrated in the following experimental studies, and the performance of the TFARMA damage index will be compared with traditional EMI damage detection techniques based on RMSD and CC damage indices to demonstrate the superiority of the proposed approach.

4. Impedance measurement in time domain

The frequency domain impedance from PZT transducers are measured by different electrical circuits, as presented by Yang *et al*. (2005). The normal impedance analyzers may not provide the time domain impedance measurement (Song *et al.* 2013), so that a new experimental measurement system is developed in this study based on the circuit proposed by Baptista *et al*. (2009) to excite the transducer and obtain the corresponding time domain impedance response.

The experimental measurement system design in this study is shown in Fig. 2. This is a new system proposed to measure the time domain impedance signal of PZT. The excitation signal is expressed as *x(t)* and the time domain response from PZT is denoted as *y(t)*. The output *y(t)* will be varying with the impedance of the PZT transducer. The resistance *Rs* is chosen by taking into account of both the PZT material specification and the amplitude of the excitation signal *x(t)*. Labview-based impedance analyzing software is used to control the impedance analyzer to generate the excitation signal *x(t)* and record the response signal *y(t)*. The excitation signal *x(t)* is a sweep frequency signal, generated by the impedance analyzer. The impedance converter network analyzer EVAL-AD5933EB from Analog Devices is used in the experimental tests. This impedance analyzer can measure the electrical impedance from 10 to 100 KHz. Based on the experiences of the sensitive frequency range of PZT impedance methods (Park *et al*. 2000), the frequency range of the excitation signal *x(t)* is defined from 40kHz to 60kHz. The magnitude and phase of impedance signals from PZT transducer are collected. The time domain impedance response *y(t)* is recorded by a National Instruments data acquisition device (NI 9215). The communication between the DAQ device and computer is through the USB connection. In this paper, the measured time domain impedances will be analyzed with the TFARMA model, and used for calculating the damage index as shown in Eq. (19).

5. Experimental validation

5.1 Experimental setup

The impedance based structural health monitoring methods are widely and successfully applied in the monitoring of civil structures, such as beam and plate-like structures. Truss bridge represents a main bridge type on highways and roads, and gusset plates in such bridges play a significant role in ensuring the rigidity and load-carrying capacity of the bridges. The gusset plate in steel truss bridges is the target area for the damage detection and condition monitoring in this study.

A simplified truss bridge model was fabricated in the laboratory as shown in Fig. 3 for the experimental tests to validate the effectiveness and performance of the proposed damage detection approach. The truss bridge model consists of four equal angles to serve as beams, a number of steel plate bar members as chords and some gusset plates at joint locations as connections. M6 bolts are used to connect all the chord members and gusset plates to the equal angles. More than 300 bolts are used in the whole bridge model. The length, width and height of the bridge model are 2 m, 0.5 m and 0.5 m, respectively. The gusset plate in the central bottom of the model is selected as the target area to place PZT transducers and perform condition monitoring. Measured impedance responses from those PZT transducers are used for the damage detection of the loosen bolts in the gusset plate, which is the main focus of this study.

Four PZT transducer patches of PSI-5H4E $(20\times 20\times 0.75mm)$ were bonded on the testing gusset, and the numbering of the placed sensors is shown in Fig. 4. They are denoted as PZT 1, PZT 2, PZT 3 and PZT 4, respectively. During the testing, the impedance analyzer will excite the PZT transducer separately to generate a small deformation on the truss bridge model. The vibration of local area on the truss model bridge will be transferred back to the PZT transducer, and the impedance signal is measured. The local damage is simulated by removing specific bolts in the target gusset plate. In this study, two bolts, as marked in Fig. 4 with two circles, connecting the vertical chord member and the target gusset plate were removed to simulate a local damage in the gusset plate. PZT 1 was located 10mm down from the locations of the introduced damages. PZT 2 and PZT 3 were placed 80mm away from the damages and on the left and right sides of the damaged locations, respectively. It is noted that PZT 1, PZT 2 and PZT 3 were all bonded on the surface of the gusset plate. However, PZT 4 was bonded on the vertical chord member and 100mm away from the locations of local damages.

A 500 ohms resistor was used to form the electric measurement circuit as shown in Fig. 2 to measure the time domain impedance. As described in Section 4, those PZT transducers were excited by the AD5933 impedance analyzer, and both the frequency and time domain impedance signals were collected by using the impedance analyzer and NI data acquisition device, respectively.

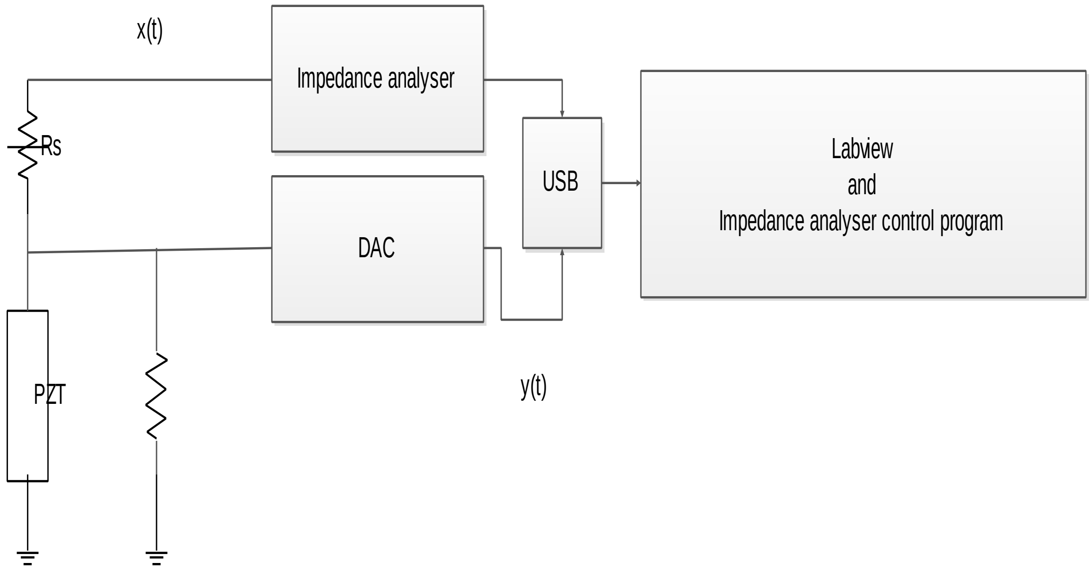

Fig. 2 Experimental measurement system design in this study

Fig. 3 The tested truss bridge model

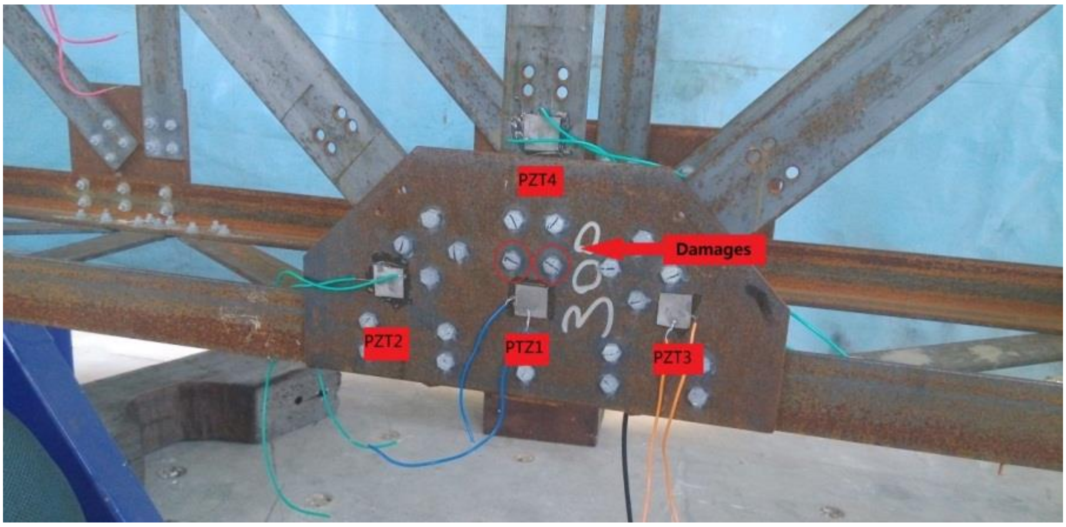

Fig. 4 The placed PZT sensors

5.2 Damage detection with traditional damage indices

The measured impedance signals in the frequency domain from healthy and damaged bridge models at each PZT transducer are shown in Fig. 5. A high frequency band from 40 kHz – 60 kHz is selected as mentioned above. It can be seen that some differences are observed specially at the peak impedance responses when the local damage is introduced. Qualitative damage diagnosis with the traditional EMI based methods is conventionally implemented by computing a scalar damage index. RMSD anc CC damage indices calculated with Eqs. (2) and (3) are two of such scalar damage indicators, and the damage index values at those four PZT patches are computed with the measured frequency impedances from the undamaged and damaged structrues.

5.3 Damage detection based on TFARMA model

The proposed damage detection method based on TFARMA model performs a two-dimensional analysis with the measured time domain impedance response, which could give a different perspective to look at the damage detection in gusset plates of truss bridges. The TFARMA model could indicate the feature and pattern of the varying process of impedance signals in the time–frequency space. The measured time domain impedance signal with the system design as shown in Fig. 3 consists of the response signals under the sweeping excitations and the standby noise signals before and after the sweeping process. One typical measured time domain impedance from PZT1 under the healthy state is shown in Fig. 6. Only the signals in the red window denote the measured time response under the sweeping excitations. The signals on the both sides of the red window are the output from the impedance analyzer in the standby mode. TFARMA model will be only built for the selected period under the sweeping excitations.

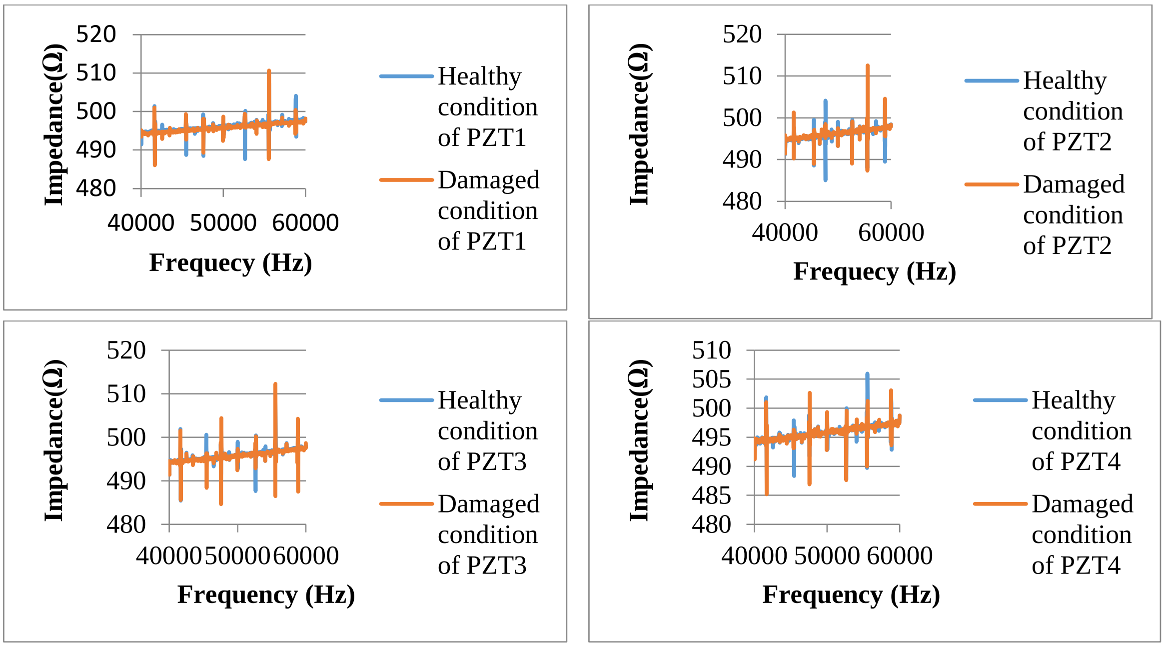

Fig. 5 Comparison of impedance signals from healthy and damaged bridge models

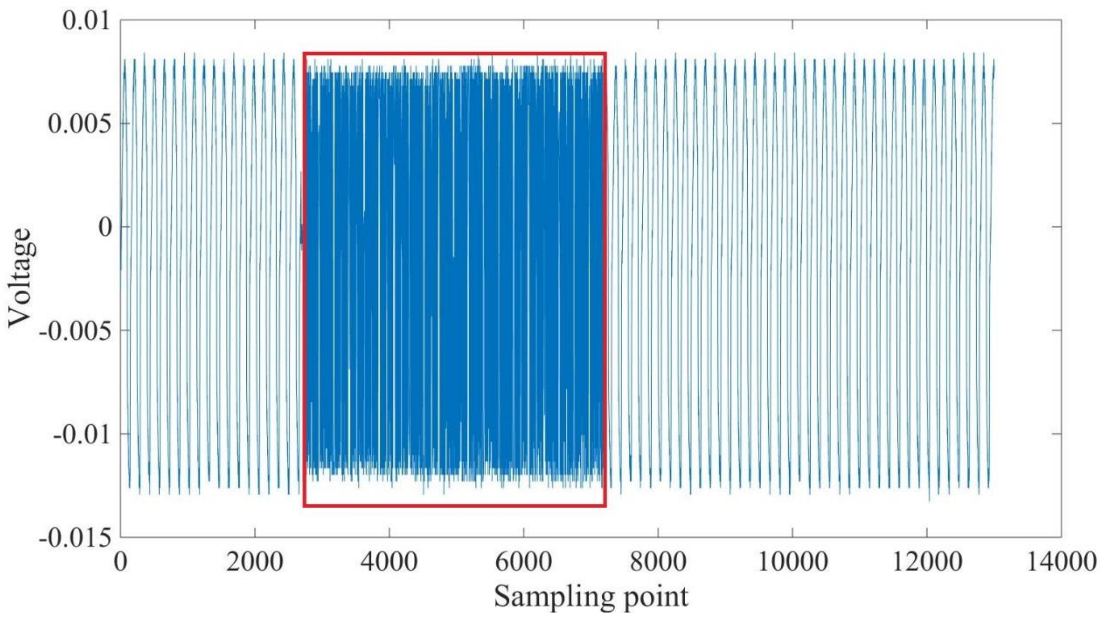

Fig. 6 Measured time domain impedance from PZT1 under the healthy condition

The TFARMA model parameters of the time domain impedance signals are estimated from the procedures and algorithms presented in Section 3.1. The evolutionary spectrum for all the four PZT patches are calculated with Eq. (15) and shown in Figs. 7-10. The difference in the number of sampling points from different cases is caused by the excitation signal generating process by the impedance analyzer. To ensure the synchronization of the frequency domain impedance signal collected by the impedance analyzer and the time domain impedance signal collected by the NI data acquisition system, the output from the impedance analyzer is used as the excitation for PZT transducer, and two devices collected the response of PZT transducer simultaneously. The excitation generated from the impedance analyzer may not be able to guarantee that the interval between scanning frequencies is exactly the same in each test, and there is a slight difference in the total sampling point. However, this slight difference does not have a significant influence on the patterns of spectrums as shown in Figs. 7-10, and the same number of points from the undamaged and damaged spectra with significant patterns is used to calculate the damage index in the subsequent study.

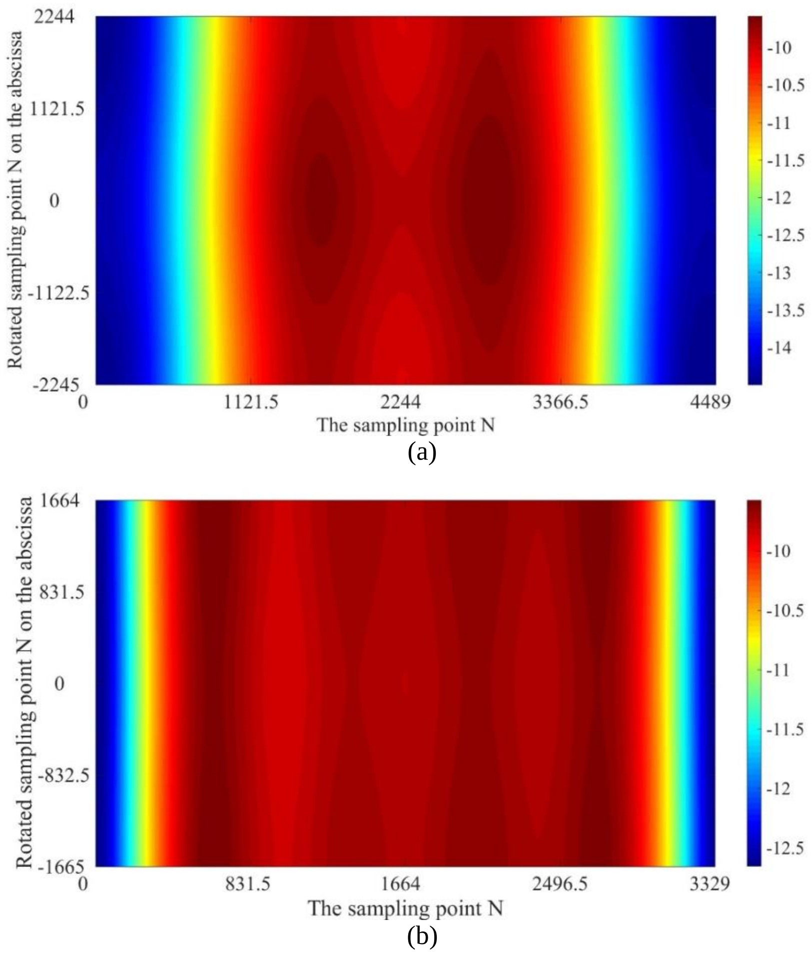

Fig. 7 The evolutionary spectra of time domain impedance signal from PZT1: (a) healthy structure and (b) damaged structure

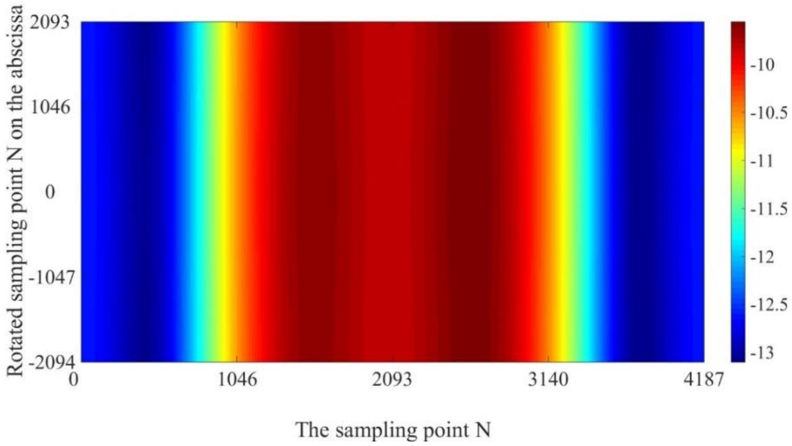

(a)

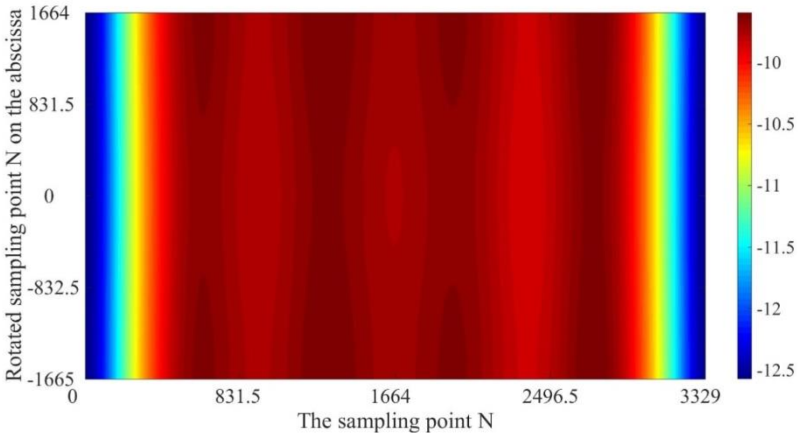

(b)

Fig. 8 The evolutionary spectra of time domain impedance signal from PZT 2: (a) healthy structure and (b) damaged structure

It is observed that the calculated spectra of the measured signals at PZT 1, PZT 2 and PZT 3 from the damaged structure as shown in Figs. 7(b), 8(b) and 9(b) consist of more than two red bands in a wide area, which has a different pattern signature as those of the healthy structure as shown in Figs. 7(a), 8(a) and 9(a). The most obvious distinction is observed at PZT 4 between the healthy spectrum and the damaged one as shown in Figs. 10(a) and 10(b), respectively. Visible and clear differences are observed in the evolutionary spectra of the signals obtained from the damaged and undamaged structure, indicating that the existence of the introduced damage may be straightforwardly detected by comparing the evolutionary spectra between the healthy and damaged states.

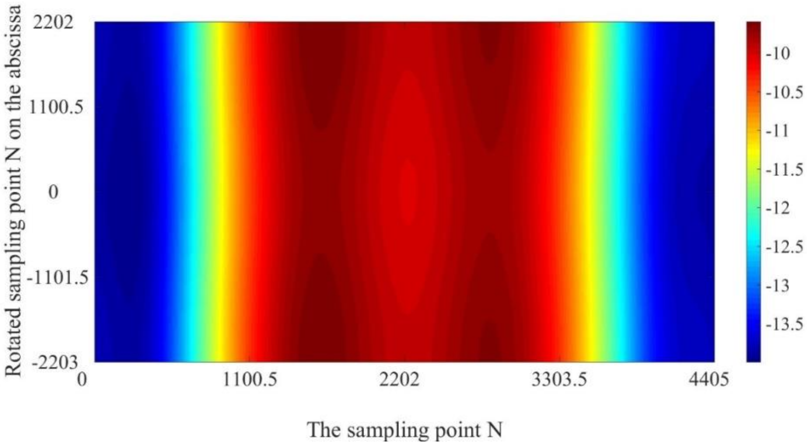

(a)

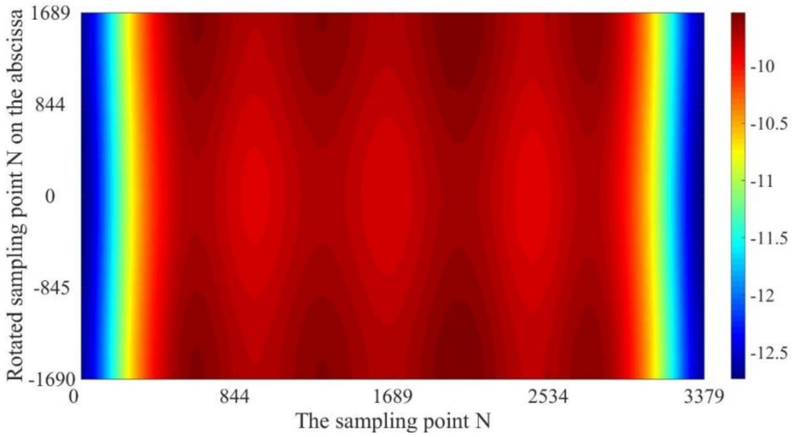

(b)

Fig. 9 The evolutionary spectra of time domain impedance signal from PZT 3: (a) healthy structure and (b) damaged structure

Based on the truss bridge design and experiment setup, the gusset plate under monitoring was fixed to all chord members by twenty-two bolts. However, the vertical chord member was bonded only by four bolts at each end. With the bolt loosen damage as shown in Fig. 4, there are still twenty bolts on the gusset plate to keep it stable. But the same damage causes a significant reduction on the holding force of the vertical chord member. The introduced damage caused a greater influence to the vertical chord member where PZT 4 is placed. This is the reason why PZT 4 has the most distinct evolutionary spectrum due to the introduced damage among all the transducers, and the identification based on TFARMA model is expected to reflect this point.

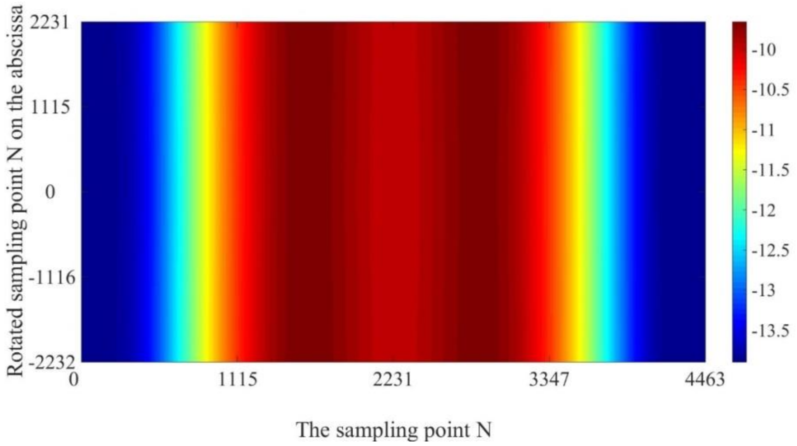

(a)

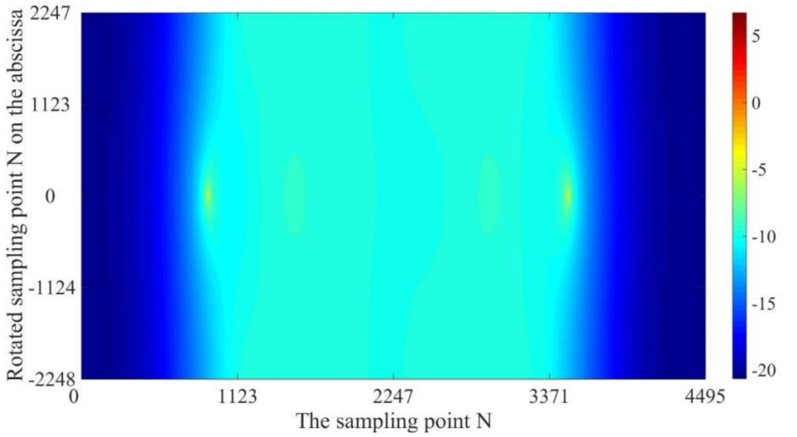

(b)

Fig. 10 The evolutionary spectra of time domain impedance signal from PZT 4: (a) healthy structure and (b) damaged structure

5.4 Comparsion among RMSD, CC and TFARMA damage indices

The TFARMA damage index is calcuated based on the obtained evolutionary spectra under the healthy and damaged states, which is used to indicate whether the proposed approach is able to identify the existence of the damage and investigate the performance and effectiveness of the proposed approach. For example, SVD is performed with the calcuated evolutionary spetrum of PZT 2 from the damaged state, and the singular values are shown in Fig. 11. Only the first ten singular values are shown. Most singular valuesare close to zero except the first one, indicating the first cloumn vector in the matrix U in Eq. (18) is the dominant one to represent the characteristics of the spectrum. Therefore the comparison between two evolutionary spectra from the healthy and damaged structures can be condcuted by using the associated first principle column vectors to calculate the TFARMA damage index in Eq. (19). The first colunm vectors used to represent the characteristics of the TFARMA evolutionary spectra of PZT 2 in the undamaged and damaged stateare shown in Fig. 12. A very different pattern in the time domain is observed indicating the proposed TFARMA could be more sensitive than the traditional one-dimensonal data analysis methods to detect the structrual damage.

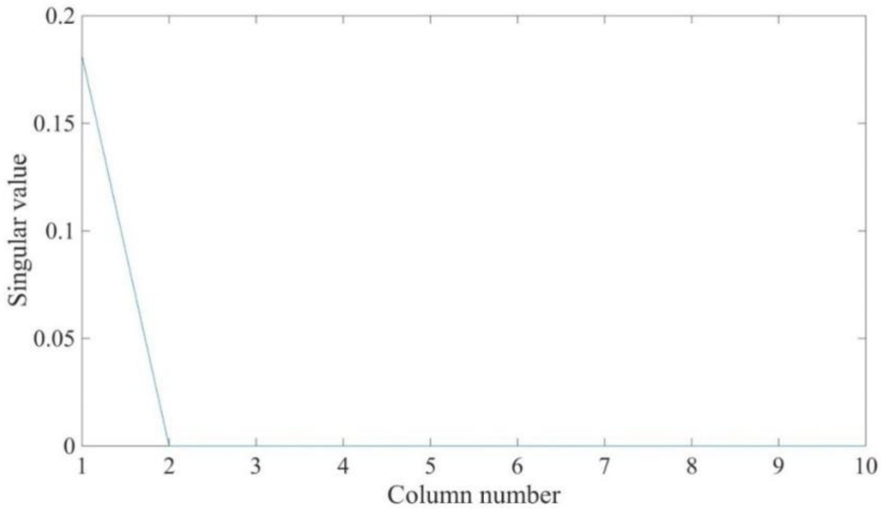

Fig. 11 The singular values of TFARMA spectrum from PZT 2 in the damaged state

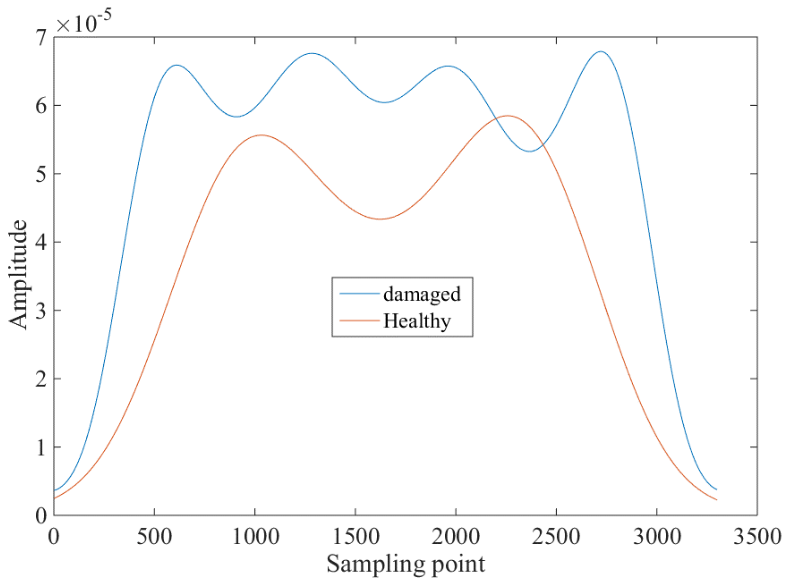

Fig. 12 The first principle column vectors of TFARMA spectra from PZT2 in the healthy and damaged states

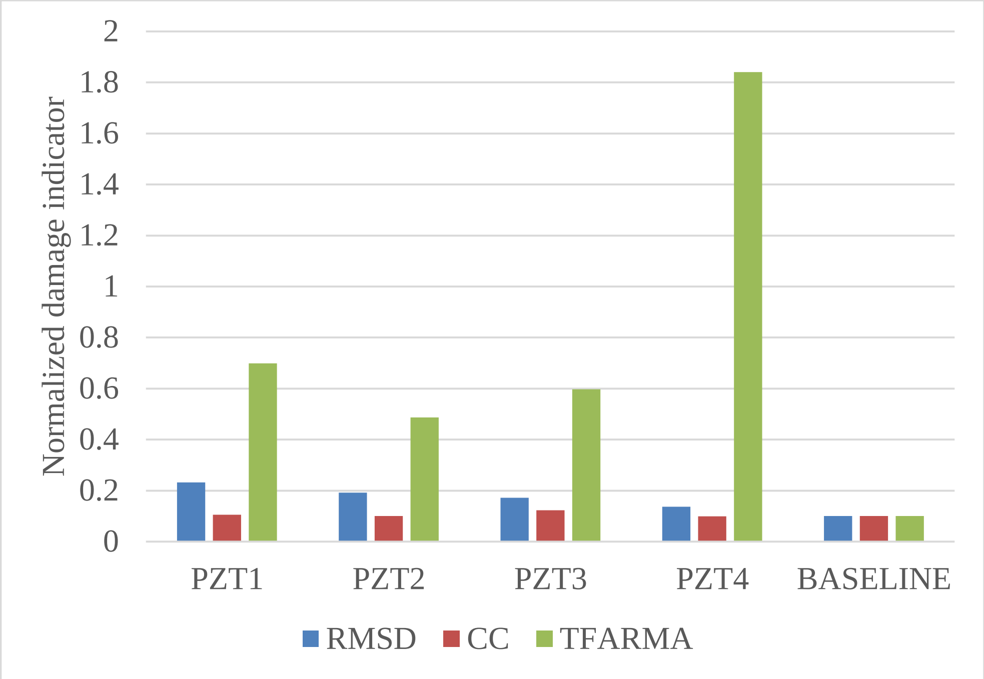

Fig. 13 Comparison of RMSD, CC and the proposed TFARMA damage index

The TFARMA damage index values at all the four PZT trransducer locations are calculated and compared with the conventional frequency impedance based damage indices, such as RMSD and CC. Fig. 13 shows the damage index values from the proposed apporach based on TFARMA model analysis and the conventional approaches based on frequency domain impedance analysis. The baseline values for the three damage indcies are set as the same value of 0.1, and the damage index values at all the four sensor locations are normalized with the baseline value for comparsion. The damage indices calcuated with two measurements from the healthy state are provided as the baseline values.

It is observed from Fig. 13 that RMSD at all the four PZT locations is able to identify the bolt loosen damage in the gusset plate of the truss bridge model. PZT 1 is the closest sensor to the damaged location, therefore it has the largest RMSD damage index value and the most sensitive performance. The RMSD damage index values of PZT 2 and PZT 3 are similar because the locations of these two transducers are symmetrical. The damage index value from PZT 4 is the smallest as it is the farest sensor to the damaged location among all the four sensors. The damage detection results with CC damage index are different from that with RMSD. The CC values from PZT 1, PZT 2 and PZT 3 are slightly higher than the baseline value. However, the CC value from PZT 4 transducer is very close to the baseline value, indicating the CC index is not capable of detecting the damage by using the measured frequency impedance data from PZT 4. Generally RMSD is observed to have a better performance than CC. Using these damage indices with a pre-defined damage threshold value from the baseline structure, the monitoring system could alarm whether any change has occurred in the monitored lcoal area. It is interesting to note that although PZT 4 is placed on the truss bar member, not on the gusset plate, it still identifies the change in the impedance and detects the damage through RMSD damage index. Note that the RMSD damage index value from PZT 4 is smaller than other three transducers, since PZT 4 was placed 100 mm from the damaged location and furthest away among all the PZT patches. The damage existence by using RMSD damage index can be detected, however, the sensitivity of such damage index depends only on the distance between the sensor and damage.

It can be seen from Fig. 13 that all the TFARMA damage indices at four PZT transducer locations are significantly higher than the baseline value, and the RMSD/CC damage index values. Similar as the detection with RMSD, the TFARMA damage index of PZT 1 has a higher value than that of PZT 2 and PZT 3 since it is closer to the damage locations. However, it is interesting to note that there is a quite large increase in the TFARMA damage index of PZT 4 compared with its RMSD damage index. The evolutionary spectra from PZT 4 as observed from Fig. 10 have the most significant and distinct difference between the undamaged and damaged states so that TFARAM damage index of PZT 4 has the largest value. It is demonstrated that PZT 4 shows a higher sensitivity than other three PZT transducers by using the proposed damage detection approach based on TFARMA model analysis.The explanation has been given in Section 5.3 because PZT 4 is placed on the vertical chord member and the other three are placed on the gusset plate. The bolt loosen damage has a significant influence to the holding force of the chord member. However, the conventional impedance based damage detection with frequency domain information only, i.e., with RMSD and CC damage indices, is not able to recognize this physical effect to the structures for damage identification. The sensitivity of RMSD and CC damage indices in frequency domain depends only on the distance between the PZT patch and the damaged location. This is because such damage indices depend only on the change in frequency response signal amplitudes therefore the sensitivity depends mainly on the distance; whereas the evolutionary spectra indicate variations not only in signal amplitudes of frequency responses, but also in time domain response pattern. The introduced damage significantly reduces the rigidity of the truss joint; therefore the signal characteristics and frequencies measured by the PZT transducer on the truss member (PZT 4) will be greatly affected. These observations demonstrate the superiority of using evolutionary spectra to detect the conditions of gusset plates when compared with the RMSD and CC damage indices. The sensitivity of using impedance responses for identifying the damage at the joint locations could be increased by examining the responses from the connected chord member with the proposed approach. However, it should be noted that the exact sensitivity radius of the proposed approach may depend on the complexity of structural model and the testing conditions.

6. Numerical verification considering a significant noise effect

Even the measured responses in the above experimental tests already include the noise effect from the environmental vibrations in the laboratory, a numerical simulation considering an extra significant noise effect is conducted to further validate the effectiveness of the proposed approach and compare the performance of TFARMA damage index with other two damage indices, i.e., RMSD and CC. A white noise is generated using Matlab and added to the original time domain impedance response. The signal-to-noise ratio is 11dB, which means the power of added noise effect is about 10% of the original signals. The noise is transformed into the frequency domain and added to the frequency domain impedance signal. Figs. 14(a) and 14(b) show respectively the time domain and frequency domain impedance signals with noise effect from PZT 1 under the damaged state.

The added noise effect could affect the effectiveness of damage detection by using the conventional approaches with frequency domain impedances and the proposed approach with time domain impedances for TFARMA analysis. The noisy responses are analyzed to obtain the RMSD, CC and TFARMA damage indices. Figs. 15(a) and 15(b) show the evolutionary spectra of PZT1 in the healthy and damaged states, respectively. It is observed that when the noise effect is included, the evolutionary spectra become slightly different from the original spectra as shown in Figs. 7(a) and 7(b).

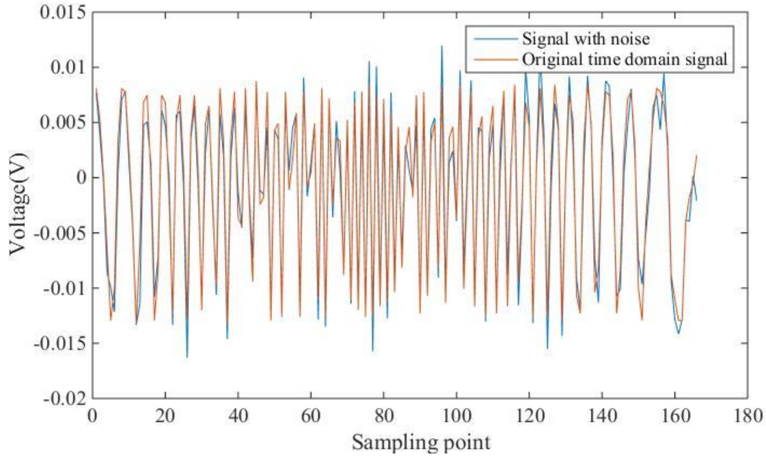

(a)

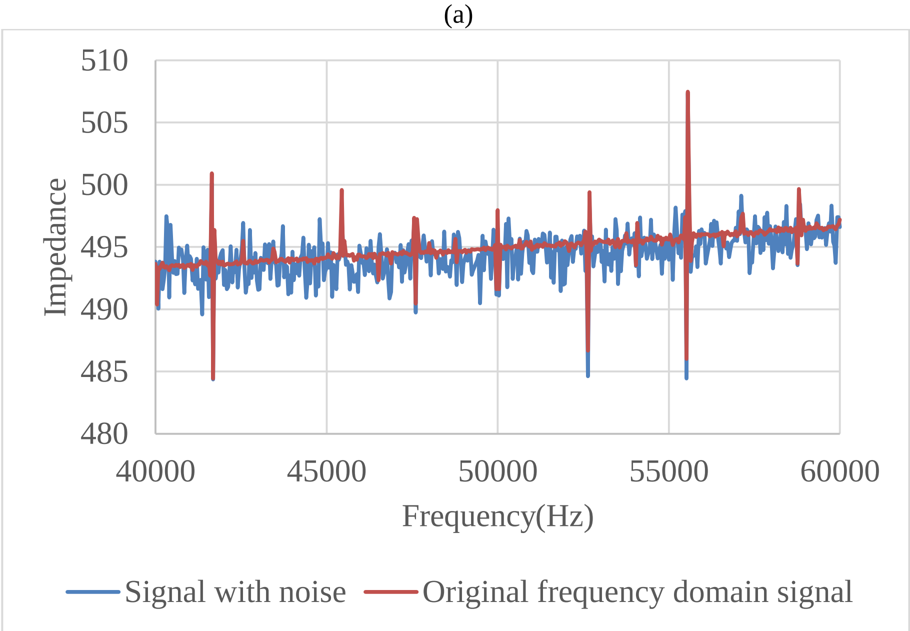

(b)

Fig. 14 Impedance signals with noise effect: (a) Time domain and (b) Frequency domain

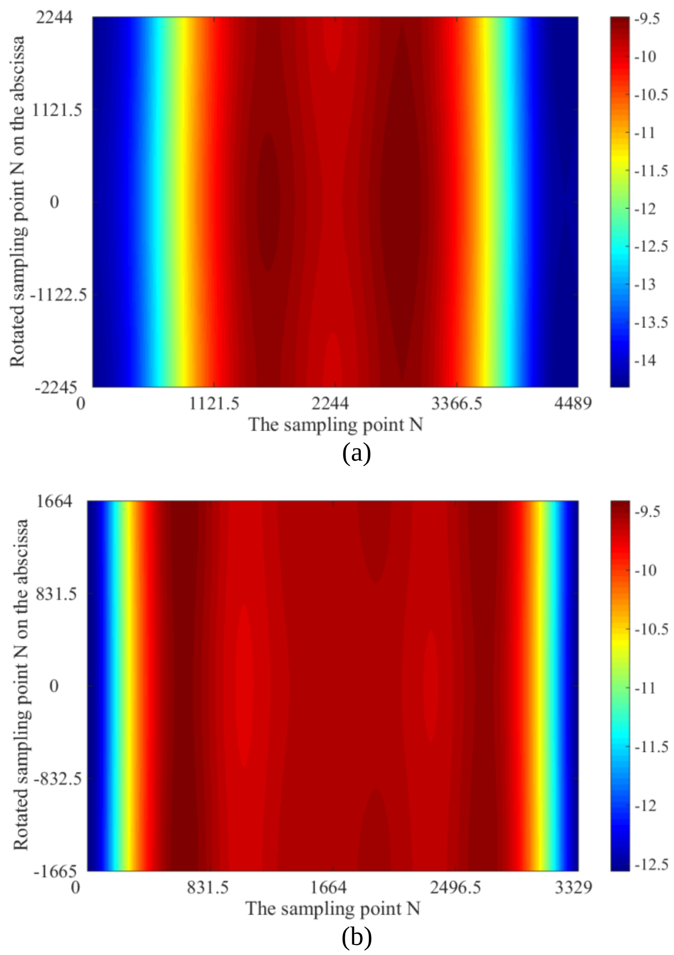

Fig. 15 The evolutionary spectra of time domain impedance signal from PZT1 with noise effect: (a) healthy structure and (b) damaged structure

The evolutionary spectra at other three sensor locations are not given due to the page limit, however, Fig. 16 shows the calculated RMSD, CC and TFARMA damage indices with noisy impedance responses. It is shown that both RMSD and CC damage indices may not be able to identify the bolt damage since their values at four PZT sensors are very close to the baseline values, indicating that the performance of RMSD and CC damage indices is biased to noise effect. However, the TFARMA damage index is still very effective to detect the damage existence with much higher damage index values compared with the baseline. It is also observed that the damage index from PZT 4 has the highest damage index value and the most sensitive performance to detect the introduced bolt damage, which is similar to the observation in Fig. 13. It is demonstrated that compared with conventional EMI based damage detection techniques with frequency domain impedances, the proposed approach based on TFARMA model analysis shows a more robust damage detection capacity and a higher sensitivity to identify the bolt damage in steel truss bridges under the noise effect.

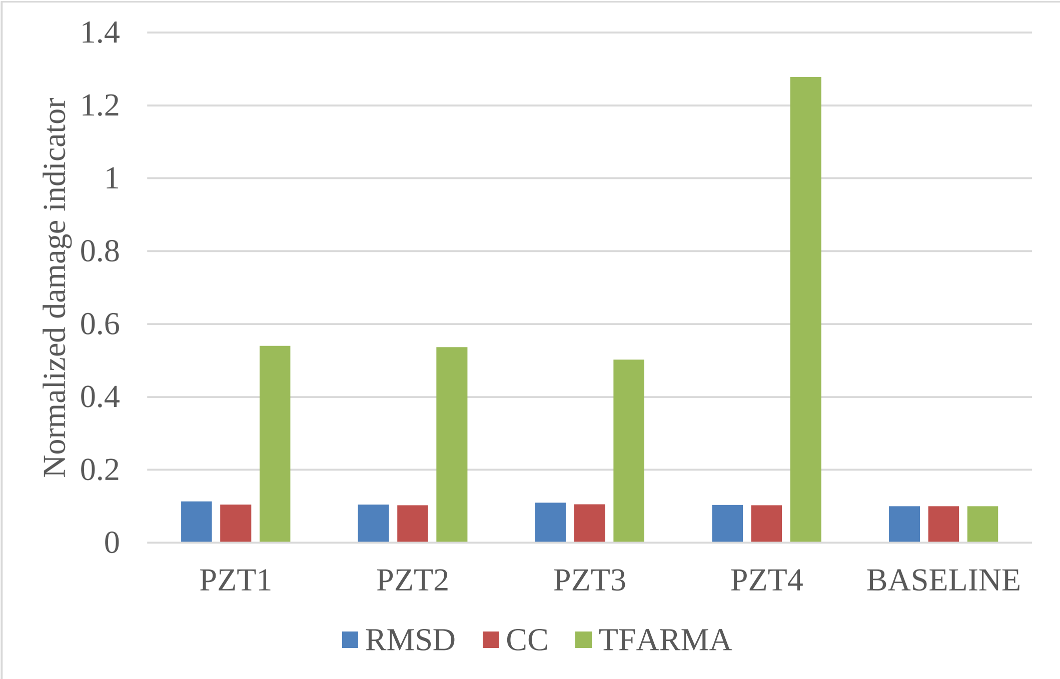

Fig. 16 Comparison of RMSD, CC and the proposed TFARMA damage index under noise effect

7. Conclusions

This paper proposes a structural damage detection approach based on analyzing the time domain impedance responses from PZT transducers for structural health monitoring of joint connections in steel truss bridges. Evolutionary spectra from TFARMA model analysis in the healthy and damaged states are used to identify the bolt loosen damage in the gusset plate. SVD is performed to analyze the evolutionary spectra and define the TFARMA damage index. The calculated TFARMA damage index is compared with other two conventional frequency domain impedance-based damage indices, i.e., RMSD and CC. The effectiveness and performance of the proposed approach are validated by experimental studies on a steel truss bridge model in the laboratory. Comparing with RMSD and CC damage indices, the TFARMA damage index shows a higher sensitivity and an improved performance to detect the bolt damage in the gusset plates of steel truss bridges. The TFARMA damage index also shows a significant improvement on the sensitivity range of using PZT transducers to identify the local damage in the targeted monitoring area by placing the PZT sensor on a different location such as the chord member connected to the gusset plate. Numerical studies with including an extra significant noise effect in the measurements demonstrate that the proposed TFARMA damage index has a more robust and reliable performance to detect the bolt damage in steel truss bridges.

Future studies may focus on investigating the possibility to identify different types of damages and the exact sensitivity radius of PZT transducers to identify the gusset plate conditions in truss bridges. Previous studies have demonstrated that the temperature effect has an influence on the impedance response signals. Efforts have been focused on developing a compensation method to remove the temperature effect, i.e., in the frequency domain impedance signal. The temperature effect is not studied in this paper, and this is a limitation of the current study. The main aim of this paper is validating the effectiveness of the proposed damage detection approach with TFARAM model and comparing the performance with the conventional frequency domain methods. Future studies will be conducted to further investigate the temperature effect on the identification accuracy of the proposed approach.

Acknowledgements

The work described in this paper was supported by Australian Research Council Discovery Early Career Researcher Award DE140101741 “Development of a Self-powered Wireless Sensor Network from Renewable Energy for Integrated Structural Health Monitoring and Diagnosis.

References

Baptista, F.G. and Filho, J.V. (2009), “A new impedance measurement system for PZT-based structural health monitoring”, IEEE *T. Instrument. Measurement*, **58**(10), 3602-3608.

Feng, Z., Liang, M. and Chu, F. (2013), “Recent advances in time–frequency analysis methods for machinery fault diagnosis: a review with application examples”, *Mech. Syst. Signal Pr.*, **38**(5), 165-205.

Jachan, M., Hlawatsch, F. and Matz, G. (2005), “Linear methods for TFARMA parameter estimation and system approximation”, *IEEE Signal Processing Workshop on Statistical Signal Array Processing*, 2; 844-852.

Jachan, M., Matz, G. and Hlawatsch, F. (2007), “Time-frequency ARMA models and parameter estimators for underspread nonstationary random processes”, *IEEE T. Signal Pr.*, **55**(9), 4366- 4381.

Li, J. and Hao, H. (2014), “Substructure damage identification based on wavelet domain response reconstruction”, *Struct. Health Monit.*, **13**(4), 389-405.

Li, J. and Hao, H. (2015), “Damage detection of shear connectors under moving loads with relative displacement measurements”, *Mech. Syst. Signal Pr.*, **60-61**, 124-150.

Li, J., Hao, H. and Zhu, H.P. (2014), “Dynamic assessment of shear connectors in composite bridges with ambient vibration measurements”, *Adv. Struct. Eng.*, **17**(5), 617-638.

Liang, C., Sun, F.P. and Rogers, C.A. (1994), “Coupled electro-mechanical analysis of adaptive material systems – determination of the actuator power consumption and system energy transfer”, *J. Intel. Mat. Syst. Str.*, **5**(1), 12-20.

Naidu, A.S.K. (2004), *Structural damage identification with admittance signatures of smart PZT transducers*, PhD Thesis, Nanyang Technological University, Singapore.

National Transportation Safety Board (2008), “Collapse of I-35W Highway Bridge Minneapolis,” Minnesota, Highway Accident Report.

Park, G., Cudney, H. and Inman, D.J. (2000), “Impedance-based health monitoring of civil structural components”, *J. Infrastruct. Syst. - ASCE*, **6**(4), 153-160.

Park, S., Lee, J.T., Yun, C.B. and Inman, D.J. (2008), “Electro-mechanical impedance-based wireless structural health monitoring using PCA-data compression and k-means clustering algorithms”, *J. Intel. Mat. Syst. Str.*, **19**(4), 509-520

Park, S., Yun, C.B., Roh, Y. and Lee, J.J. (2005), “Health monitoring of steel structures using impedance of thickness modes at PZT patches”, *Smart Struct. Syst.*, **1**(4), 339-353.

Pavelko, I., Pavelko, V., Kuznetsov, S. and Ozolinsh, I. (2014), “Bolt-joint structural health monitoring by the method of electromechanical impedance”, *Aircraft Eng. Aerospace Technol.*, **86**(3), 207-214.

Raju, V., Park, G. and Cudney, H. (1998), “Impedance-based health monitoring technique of composite

reinforced structures", *Proceedings of the 9th International Conference on Adaptive Structures and Technologies*.
Rucka, M. and Wilde, K. (2006), "Application of continuous wavelet transform in vibration based damage detection method for beams and plates", *J. Sound Vib.*, **297**(3-5), 536-550.
Sohn, H., Allen, D.W., Worden, K. and Farrar, C.R. (2003), "Statistical damage classification using sequential probability ratio tests," *Struct. Health Monit.*, **2**(1), 57-74.
Song, H., Lim, H.J. and Sohn, H. (2013), "Electromechanical impedance measurement from large structures using a dual piezoelectric transducer", *J. Sound Vib.*, **332**(25), 6580-6595.
Stoica, P. and Moses, R. (1997), *Introduction to Spectral Analysis*, *Prentice-Hall*, 1st Edition.
Sun, R., Sevillano, E. and Perera, R. (2015), "Debonding detection of FRP strengthened concrete beams by using impedance measurements and an ensemble PSO adaptive spectral model", *Compos. Struct.*, **125**, 374-387.
Tseng, K.K.H. and Naidu, A.S.K. (2002), "Non-parametric damage detection and characterization using smart piezoceramic material", *Smart Mater. Struct.*, **11**(3), 317-329.
Wang, D., Song, H. and Zhu, H. (2014), "Embedded 3-D electromechanical impedance model for strength monitoring of concrete using PZT transducer", *Smart Mater. Struct.*, **23**(11), 115019.
Wang, D., Zhu, H., Chen, C. and Xia, Y. (2007), "An impedance analysis for crack detection in the Timoshenko beam based on the anti-resonance technique", *Acta Mech. Solida Sinica*, **20**(3), 228-235.
Wax, M. and Kailath, T. (1983), "Efficient inversion of Toeplitz-block Toeplitz matrix", *IEEE T. Acoust., Speech Signal Pr.*, **31**(5), 1218-1221.
Yang, J.N., Lei, Y., Lin, S. and Huang, N. (2004), "Hilbert-Huang based approach for structural damage detection", *J. Eng. Mech. - ASCE*, **130**(1), 85-95.
Yang, J.N., Lei, Y., Pan, S. and Huang, N. (2003), "System identification of linear structures based on Hilbert-Huang spectral analysis Part 1: Normal modes", *Earthq. Eng. Struct. D.*, **32**(9), 1443-1467.
Yang, Y.W., Xu, J.F. and Soh, C.K. (2005), "Generic impedance-based model for structure-piezoceramic interacting system", *J. Aerospace Eng. - ASCE*, **18**(2), 93-101.
Yi, T.H., Li, H.N. and Gu, M. (2013a), "Wavelet based multi-step filtering method for bridge health monitoring using GPS and accelerometer", *Smart Struct. Syst.*, **11**(4), 331-348.
Yi, T.H., Li, H.N. and Sun, H.M. (2013b), "Multi-stage structural damage diagnosis method based on "energy-damage" theory", *Smart Struct. Syst.*, **12**(3), 345-361.